EURASIP Journal on Applied Signal Processing 2005:15, 2426–2436

Detection of Point Sources on Two-Dimensional Images Based on Peaks

M. López-Caniego
Instituto de Física de Cantabria, CSIC-Universidad de Cantabria, and Departamento de Física Moderna, Universidad de Cantabria, avenida de los Castros s/n, 39005 Santander, Spain
Email: caniego@ifca.unican.es

D. Herranz
Istituto di Scienze e Tecnologie dell'Informazione "A. Faedo," CNR, via Moruzzi 1, 56124 Pisa, Italy
Email: herranz@ifca.unican.es

J. L. Sanz
Instituto de Física de Cantabria, CSIC-Universidad de Cantabria, avenida de los Castros s/n, 39905 Santander, Spain
Email: sanz@ifca.unican.es

R. B. Barreiro
Instituto de Física de Cantabria, CSIC-Universidad de Cantabria, avenida de los Castros s/n, 39905 Santander, Spain
Email: barreiro@ifca.unican.es

Received 8 June 2004; Revised 7 February 2005

This paper considers the detection of point sources in two-dimensional astronomical images. The detection scheme we propose is based on peak statistics. We discuss the example of the detection of far galaxies in cosmic microwave background experiments throughout the paper, although the method we present is totally general and can be used in many other fields of data analysis. We consider sources with a Gaussian profile—that is, a fair approximation of the profile of a point source convolved with the detector beam in microwave experiments—on a background modeled by a homogeneous and isotropic Gaussian random field characterized by a scale-free power spectrum. Point sources are enhanced with respect to the background by means of linear filters. After filtering, we identify local maxima and apply our detection scheme, a Neyman-Pearson detector that defines our region of acceptance based on the a priori pdf of the sources and the ratio of number densities. We study the different performances of some linear filters that have been used in this context in the literature: the Mexican hat wavelet, the matched filter, and the scale-adaptive filter. We consider as well an extension to two dimensions of the biparametric scale-adaptive filter (BSAF). The BSAF depends on two parameters which are determined by maximizing the number density of real detections while fixing the number density of spurious detections. For our detection criterion the BSAF outperforms the other filters in the interesting case of white noise.

Keywords and phrases: analytical methods, data analysis methods, image processing techniques.

1. INTRODUCTION

A very challenging aspect of data analysis in astronomy is the detection of pointlike sources embedded in one- and two-dimensional images. Some common examples are the separation of individual stars in crowded optical images, the identification of emission and absorption lines in noisy one-dimensional spectra, and the detection of faint extragalactic objects at microwave frequencies. This latter case, for example, is one of the most critical issues for the new generation of experiments that observe the cosmic microwave background (CMB).

The CMB is the remnant of the radiation that filled the universe immediately after the big bang. This weak radiation can provide us with answers to one of the most important set of questions asked in modern science—how the universe did begin, how it evolved to the state we observe today, and how it will continue to evolve in the future. Unfortunately, we do not measure the CMB alone but a mixture of it with instrumental noise and other astrophysical radiations that are usually referred to as *foregrounds*.

Some foregrounds are due to our own galaxy, for example, the thermal emission due to dust grains in the galactic plane or the synchrotron emission by relativistic electrons

moving along the galactic magnetic field. These foregrounds appear as diffuse emission in the sky, and their spectral behaviors (the way the emission scales from one wavelength of observation to another) are reasonably well known. Another foreground with a well-known spectral behavior is the Sunyaev-Zel'dovich effect, which is due to the hot gas contained in galaxy clusters that distorts the energy distribution of CMB photons. Foreground emissions carry information about the galaxy structure, composition, and physical parameters as well as about the number, distribution, and evolution of galaxy clusters that map the distribution of matter in the universe. Therefore, the study of the different foregrounds has great scientific relevance by itself. In order to properly study the CMB and the different foregrounds, it is mandatory to *separate* the signals (*components*) that are mixed in the observations. This can be done by observing the sky at a number of frequencies at least as big as the number of components and then applying some statistical *component separation* method in order to recover the different astrophysical signals. Several component separation techniques have been suggested, including blind (Baccigalupi et al. [1], Maino et al. [2], Delabrouille et al. [3]), semi-blind (Bedini et al. [4]) and nonblind (Hobson et al. [5], Bouchet and Gispert [6], Stolyarov et al. [7], Barreiro et al. [8]) approaches.

Another important foreground is due to the emission of far galaxies. Since the typical angular size of the galaxies in the sky is a few arcseconds and the angular resolution of the microwave detectors is typically greater than a few arcminutes,[1] galaxies appear as points to the detector, which is unable to resolve their inner structure. Therefore, they are usually referred to as *extragalactic point sources* (EPS) in the CMB jargon. Note that, however, they do not appear as points in the images but as the convolution of a pointlike impulse with the angular response of the detector (*beam*). The instruments (radiometers and bolometers) that are used in CMB experiments have angular responses that are approximately Gaussian and therefore EPS appear as small Gaussian (or nearly Gaussian) spots in the images.[2]

The problem with EPS is that galaxies are a very heterogeneous bundle of objects, from the radio galaxies that emit most of their radiation in the low-frequency part of the electromagnetic spectrum to the dusty galaxies that emit mainly in the infrared (Toffolatti et al. [9], Guiderdoni et al. [10], Tucci et al. [11]). This makes it impossible to consider all of them as a single foreground to be separated from the other by means of multiwavelength observations and statistical component separation techniques. EPS constitute an important contaminant in CMB studies at small angular scales (Toffolatti et al. [9]), affecting the determination of the CMB angular power spectrum and hampering the statistical study (e.g., the study of Gaussianity) of CMB and other foregrounds at such scales. Moreover, while there are good galaxy surveys at radio and infrared frequencies, the microwave window of the electromagnetic spectrum is a practically unknown zone for extragalactic astronomy. Therefore, it is important to have detection techniques that are able to detect EPS with fluxes as low as possible.

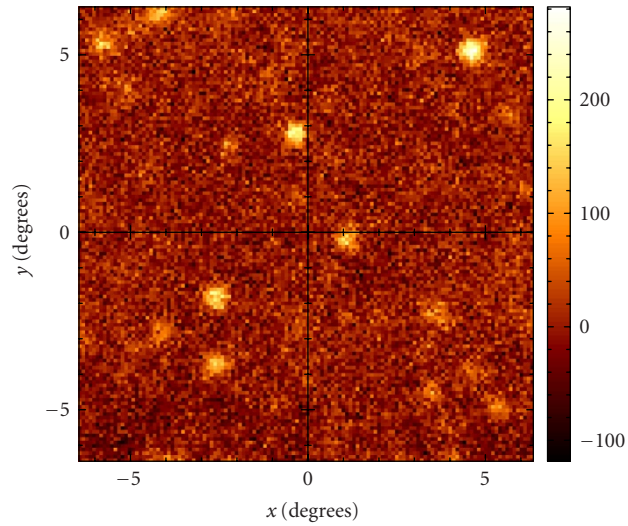

Figure 1: Residual map of a 12.8×12.8 square degrees sky patch at 30 GHz after the application of a maximum entropy component separation. The residual map is obtained by subtracting from the 30 GHz map the different components (CMB and foregrounds) given by the maximum entropy algorithm. Bright point sources appear as spots in the images whereas faint point sources are masked by the residual noise.

One possibility is to consider the EPS emission at each frequency as an additional noise to be considered in the equations of a statistical component separation method. Once the algorithm has separated the different components, the residual that is obtained by subtracting the output foregrounds from the original data should contain the EPS plus the instrumental noise and some amount of foreground residuals that remain due to a nonperfect separation. As an example, Figure 1 shows the residual at 30 GHz after applying a maximum entropy component separation algorithm (Hobson et al. [12]) to a 12.8×12.8 square degrees simulated sky patch as would be observed by the Planck satellite. The brightest point sources can be clearly observed over the residual noise. However, fainter point sources are still masked by a residual noise that is approximately Gaussian and must be detected somehow. Besides, the situation is more complex because the presence of bright EPS in the data affects the performance of the component separation algorithms so the recovered components are contaminated by point sources in a way that is difficult to control. Therefore, any satisfactory method should detect and extract at least the bright sources before the component separation. Then, after separation some additional low intensity EPS could be detected from the residual maps such as the one in Figure 1.

[1] For example, the upcoming ESA's Planck satellite will have angular resolutions ranging from 5 arcminutes (for the 217–857 GHz channels) to 33 arcminutes (for the 30 GHz channel).

[2] It is also common to speak of *compact sources*, describing a source that is comparable to the size of the beam being used. Non-pointlike sources (such as large galaxy clusters with arcminute angular scales) will have more complicated responses when convolved with a beam, but if the source profile is known, it is always possible to apply the methods presented in this work.

Several techniques based on linear filters have been proposed in the literature for the detection of point sources in CMB data. Linear filtering techniques are suitable for this problem because they can isolate structures with a given characteristic scale, as is the case of pointlike sources, while canceling the contribution of diffuse foregrounds. Among the methods proposed in the literature, we emphasize the Mexican hat wavelet (MHW, Cayón et al. [13], Vielva et al. [14, 15, 16]), the classic *matched filter* (MF, Tegmark and de Oliveira-Costa [17]), the adaptive top hat filter (Chiang et al. [18]), and the scale-adaptive filter (SAF, Sanz et al. [19], Herranz et al. [20]). Moreover, linear filters can be used in combination with statistical component separation techniques in order to produce a more accurate separation of the different foregrounds (Vielva et al. [15]).

The goal of filtering is to enhance the contrast between the source to be detected and the background that masks it. For example, if we filter the image in Figure 1, assuming that the background can be characterized by a white noise, with the well-known matched filter (see Section 4.1) at the scale of the 30 GHz detector beam (FWHM = 33 arcminutes) the signal-to-noise ratio of the sources increases by more than 25%. Therefore, a source whose signal-to-noise ratio was ~ 3 before filtering becomes a source with signal-to-noise ratio ~ 4 and will be easier to detect.

After filtering, a *detection rule* is applied to the data in order to decide whether the source is present or not. The usual detection approach in astronomy is *thresholding*: for any given candidate (e.g., a local peak in the data), a positive detection is considered if the candidate has a signal-to-noise ratio greater than a certain threshold (in many astronomical applications, a typical value of this threshold is 5σ). This naive approach works fine for bright sources, but weak sources can be easily missed.

More sophisticated detection schemes can use additional information in order to improve the detection. If the detection is performed by means of the study of the statistics of maxima in the images, such information includes not only the amplitude of the maxima but also spatial information related to the source profile, for example, the derivatives of the intensity. In our approach we will consider the amplitude, the curvature, and the shear of the sources (the last two quantities are given by the properties of the beam in the case of point sources) to discriminate between maxima of the background and real sources. Moreover, in some cases a priori information on the distribution of intensity of the sources is known. We will therefore use a Neyman-Pearson detector that uses the three above-mentioned elements of information (amplitude, curvature, and shear) of the maxima as well as the a priori probability distribution of the sources. This technique has been successfully tested in images of one-dimensional fields (López-Caniego et al. [21, 22]). In this work we will generalize it to two dimensions.

The overview of this work is as follows. In Section 2 we describe the statistics of the peaks for a two-dimensional Gaussian background in the absence and presence of a source. In Section 3 we introduce the detection problem, define the region of acceptance, and derive our detector. In Section 4 we briefly review some of the linear filters proposed in the literature. In Section 5 we describe a probability distribution of sources that is of interest and compare the performance of the filters, regarding our choice of detector. Finally, in Section 6 we summarize our results.

2. PEAK STATISTICS

In this section we will study the statistics of peaks for a two-dimensional Gaussian background in both the absence and presence of a source. We will focus on three quantities that define the properties of the peaks: the intensity of the field, the curvature, and the shear at the position of the peak. The first quantity gives the amplitude of the peak. The curvature and the shear give information about the spatial structure of the peak and are related to its sharpness and eccentricity, respectively.

2.1. Background

We consider a two-dimensional (2D) background represented by a Gaussian random field $\xi(\vec{x})$ with average value $\langle \xi(\vec{x}) \rangle = 0$ and power spectrum $P(q)$,

$$\langle \xi(\vec{Q}) \xi^*(\vec{Q'}) \rangle = P(q) \delta_D^2(\vec{Q} - \vec{Q'}), \quad q \equiv |\vec{Q}|, \tag{1}$$

where $\xi(\vec{Q})$ is the Fourier transform of $\xi(\vec{x})$[3] and δ_D^2 is the Dirac distribution in 2D.

We are interested in the distribution of maxima of the background with respect to the three variables already mentioned: intensity, curvature, and shear. We define the *normalized field intensity* ν, the *normalized curvature* κ, and the *normalized shear* ϵ as

$$\nu \equiv \frac{\xi}{\sigma_0}, \qquad \kappa \equiv \frac{\lambda_1 + \lambda_2}{\sigma_2}, \qquad \epsilon \equiv \frac{\lambda_1 - \lambda_2}{2\sigma_2}, \tag{2}$$

where $\nu \in (-\infty, \infty)$, $\kappa \in [0, \infty)$, $\epsilon \in [0, \kappa/2)$, λ_1 and λ_2 are the eigenvalues of the negative Hessian matrix, and the σ_n are defined as

$$\sigma_n^2 \equiv \frac{1}{2\pi} \int_0^\infty dq\, q^{1+2n} P(q). \tag{3}$$

The moment σ_0 is equal to the dispersion of the field.

The distribution of maxima of the background in one dimension (1D) with respect to the intensity and curvature (the shear is not defined in 1D) was studied by Rice [23]. If we generalize it to 2D, including the shear, the expected

[3] Throughout this paper we will use the following notation for the Fourier transform: the same symbol will be used for the real space and the Fourier space versions of a given function. The argument of the function will specify in each case which is the space we are referring to. For instance, $f(q)$ will be the Fourier transform of the function $f(x)$.

number density of maxima per intervals $(\vec{x}, \vec{x}+d\vec{x})$, $(\nu, \nu+d\nu)$, $(\kappa, \kappa+d\kappa)$, and $(\epsilon, \epsilon+d\epsilon)$ is given by

$$n_b(\nu,\kappa,\epsilon) = \frac{8\sqrt{3}\tilde{n}_b}{\pi\sqrt{1-\rho^2}}\epsilon(\kappa^2-4\epsilon^2)e^{-(1/2)\nu^2-4\epsilon^2-(\kappa-\rho\nu)^2/2(1-\rho^2)}, \tag{4}$$

where $\tilde{n}_b$ is the expected total number density of maxima (i.e., number of maxima per unit area $d\vec{x}$),

$$\tilde{n}_b \equiv \frac{1}{4\pi\sqrt{3}\theta_m^2}, \tag{5}$$

and ρ and θ_m are defined as

$$\theta_m \equiv \sqrt{2}\frac{\sigma_1}{\sigma_2}, \qquad \rho \equiv \frac{\sigma_1^2}{\sigma_0\sigma_2} = \frac{\theta_m}{\theta_c}, \quad \theta_c \equiv \sqrt{2}\frac{\sigma_0}{\sigma_1}. \tag{6}$$

In the previous equations θ_c and θ_m are the coherence scale of the field and maxima, respectively. The formula in (4) can be derived from previous works (Bond and Efstathiou [24], Barreiro et al. [25]).

2.2. Background plus point source

To the previous 2D background we add a source with a known spatial profile $\tau(\vec{x})$ and an amplitude A, so that the intensity due to the source at a given position $\vec{x}_0$ is $\xi_s(\vec{x}) = A\tau(\vec{x}-\vec{x}_0)$. For simplicity, we will consider a spherical Gaussian profile given by

$$\tau(x) = \exp\left(-\frac{x^2}{2R^2}\right), \quad x \equiv |\vec{x}|, \tag{7}$$

where R is the Gaussian width (in the case of point sources convolved with a Gaussian beam, R is the beam width). We could easily consider other functional profiles[4] without any loss of generality. The expected number density of maxima per intervals $(\vec{x}, \vec{x}+d\vec{x})$, $(\nu, \nu+d\nu)$, $(\kappa, \kappa+d\kappa)$, and $(\epsilon, \epsilon+d\epsilon)$, given a source of amplitude A in such spatial interval, is

$$n(\nu,\kappa,\epsilon|\nu_s) = \frac{8\sqrt{3}\tilde{n}_b}{\pi\sqrt{1-\rho^2}}\epsilon(\kappa^2-4\epsilon^2)e^{-(1/2)(\nu-\nu_s)^2-4\epsilon^2-(\kappa-2\kappa_s-\rho(\nu-\nu_s))^2/2(1-\rho^2)}, \tag{8}$$

where $\nu_s = A/\sigma_0$ is the normalized amplitude of the source, $\kappa_s = -A\tau''/\sigma_2$ is the normalized curvature of the source, and τ'' is the second derivative of the source profile τ with respect to x at the position of the source. Note that in (8) we are taking into account that the shear of the source is zero since we are considering a spherical profile. It is useful to define a quantity y_s that is related to the curvature of the source:

$$y_s \equiv -\frac{\theta_m^2\tau''}{\rho}, \qquad \kappa_s = \frac{\nu_s y_s}{2}. \tag{9}$$

[4] For example, more complicated beams or sources that are not pointlike but have some resolved structure.

3. THE DETECTION PROBLEM

Equations (4) and (8) can be used to decide whether a source is present or not in a data set. The tool that allows us to decide whether a point source is present or not in the data is called a *detector*. In this section we will describe the Neyman-Pearson detector (NPD). We will study its performance in terms of two quantities: the number of true detections and the number of false (spurious) detections that emerge from the detection process. Our approach fixes the number density of spurious detections and determines the number density of true detections in each case.

3.1. The region of acceptance

We consider a peak in the 2D dataset characterized by the normalized amplitude, curvature, and shear (ν, κ, ϵ). The number density of background maxima $n_b(\nu,\kappa,\epsilon)$ represents the null hypothesis H_0 that the peak is due to the background in the absence of source. Conversely, the local number density of maxima $n(\nu,\kappa,\epsilon)$ represents the alternative hypothesis, that the peak is due to the source added to the background. The local number density of maxima $n(\nu,\kappa,\epsilon)$ can be calculated as

$$n(\nu,\kappa,\epsilon) = \int_0^\infty d\nu_s\, p(\nu_s)\, n(\nu,\kappa,\epsilon|\nu_s). \tag{10}$$

In the last equation we have used the a priori probability $p(\nu_s)$ that gives the amplitude distribution of the sources.

We can associate to any region $\mathcal{R}_*(\nu,\kappa,\epsilon)$ in the (ν,κ,ϵ) parameter space two number densities n_b^* and n^*,

$$\begin{aligned} n_b^* &= \int_{\mathcal{R}_*} d\nu\, d\kappa\, d\epsilon\; n_b(\nu,\kappa,\epsilon), \\ n^* &= \int_{\mathcal{R}_*} d\nu\, d\kappa\, d\epsilon\; n(\nu,\kappa,\epsilon), \end{aligned} \tag{11}$$

where n_b^* is the expected number density of spurious sources, that is, due to the background, in the region $\mathcal{R}_*(\nu,\kappa,\epsilon)$, whereas n^* is the number density of maxima expected in the same region of the (ν,κ,ϵ) space in the presence of a local source. The region $\mathcal{R}_*$ will be called the *region of acceptance*.

In order to define the region of acceptance $\mathcal{R}_*$ that gives the highest number density of detections n^* for a given number density of spurious detections n_b^*, we consider a Neyman-Pearson detector (NPD) using number densities instead of probabilities

$$L(\nu,\kappa,\epsilon) \equiv \frac{n(\nu,\kappa,\epsilon)}{n_b(\nu,\kappa,\epsilon)} \geq L_*, \tag{12}$$

where L_* is a constant. The proof follows the same approach as for the standard Neyman-Pearson detector. If $L \geq L_*$ we decide that the signal is present, whereas if $L < L_*$ we decide that the signal is absent. From this ratio $L \geq L_*$, we derive the region of acceptance that is given by the sufficient linear detector φ (see appendix)

$$\mathcal{R}_* : \varphi(\nu,\kappa) \geq \varphi_*, \tag{13}$$

where φ_* is a constant and $\varphi(\nu,\kappa)$ is given by

$$\varphi(\nu,\kappa) \equiv a\nu + b\kappa, \quad a \equiv \frac{1-\rho y_s}{1-\rho^2},\ b \equiv \frac{y_s-\rho}{1-\rho^2}. \tag{14}$$

We remark that the detector is independent of the shear ϵ. This is due to the fact that we are considering a source with a spherical profile with shear $\epsilon_s = 0$. If the profile is not spherical, the detector may depend on the shear.

3.2. Spurious sources and real detections

Given a region of acceptance $\mathcal{R}_*$, we can calculate the number density of spurious sources and the number density of detections as given by (11):

$$n_b^* = \frac{\sqrt{3}\widetilde{n}_b}{\sqrt{2\pi}} \int_0^\infty d\kappa(\kappa^2 - 1 + e^{-\kappa^2})e^{-\kappa^2/2}\operatorname{erfc}(M), \qquad M \equiv \frac{\varphi_* - y_s\kappa}{a\sqrt{2(1-\rho^2)}}; \tag{15}$$

$$n^* = \frac{\sqrt{3}\widetilde{n}_b}{\sqrt{2\pi}} \int_0^\infty d\nu_s p(\nu_s) \times \int_0^\infty d\kappa(\kappa^2 - 1 + e^{-\kappa^2})e^{-(1/2)(\kappa-\nu_s y_s)^2}\operatorname{erfc}(Q), \tag{16}$$

$$Q \equiv M + \nu_s \frac{\rho y_s - 1}{\sqrt{2(1-\rho^2)}}. \tag{17}$$

Our approach is to fix the number density of spurious detections and then to determine the region of acceptance that gives the maximum number of true detections. This can be done by inverting (15) to obtain $\varphi_* = \varphi_*(n_b^*/n_b; \rho, y_s)$. Once φ_* is known, we can calculate the number density of detections using (16).

4. THE FILTERS

Detection can, in principle, be performed on the raw data, but in most cases it is convenient to transform first the data in order to enhance the contrast between the distributions $n_b(\nu,\kappa,\epsilon)$ and $n(\nu,\kappa,\epsilon)$. Hopefully, such an enhancement will help the detector to give better results (namely, a higher number of true detections). In this paper we will focus on the use of linear filters as a means to transform the data in such a way. Filters are suitable for this task because background fluctuations that have variation scales different from the source scale can be easily filtered out while preserving the sources. Different filters will improve detection in different ways: this paper compares the performance of several filters. The filter that gives the highest number density of detections, for a fixed number density of spurious sources, will be the preferred filter among the considered filters.

We consider a filter $\Psi(\vec{x}; R, \vec{b})$, where R and $\vec{b}$ define a scaling and a translation respectively. Since the sources we are considering are spherically symmetric and we assume that the background is statistically homogeneous and isotropic, we will consider spherically symmetric filters,

$$\Psi(\vec{x}; R, \vec{b}) \equiv \frac{1}{R^2}\psi\left(\frac{|\vec{x}-\vec{b}|}{R}\right). \tag{18}$$

If we filter our background with $\Psi(\vec{x}; R, \vec{b})$, the filtered field is

$$w(R, \vec{b}) = \int d\vec{x}\,\xi(\vec{x})\Psi(\vec{x}; R, \vec{b}). \tag{19}$$

The filter is normalized such that the amplitude of the source is the same after filtering:

$$\int d\vec{x}\,\tau(\vec{x})\Psi(\vec{x}; R, \vec{0}) = 1. \tag{20}$$

For the filtered field, (3) becomes

$$\sigma_n^2 \equiv 2\pi \int_0^\infty dq\, q^{1+2n} P(q)\psi^2(q). \tag{21}$$

The values of ρ, θ_m, θ_c, and all the derived quantities change accordingly. The curvature of the filtered source κ_s can be obtained through (9), taking into account that for the filtered source,

$$-\tau_\psi'' = \pi \int_0^\infty dq\, q^3 \tau(q)\psi(q). \tag{22}$$

Note that the function $\psi(q)$ will depend as well on the scaling R. As an application of the previous ideas, we study the detection of point sources characterized by a Gaussian profile $\tau(x) = \exp(-x^2/2R^2)$, $x = |\vec{x}|$, and Fourier transform $\tau(q) = R^2\exp(-(qR)^2/2)$. This is the case we find in CMB experiments, where the profile of the point source is given by the instrumental beam that can be approximated by a Gaussian.

This profile introduces in a natural way the scale of the source R, the scale at which we filter. However, previous works in 1D using the MHW, MF, SAF, and BSAF have shown that the use of a modified scale αR can significantly improve the number of detections (Cayón et al. [13], Vielva et al. [14, 15], López-Caniego et al. [21, 22]). Therefore, we generalize the functional form of these filters to 2D and allow for this additional degree of freedom α.

4.1. The matched filter

We introduce a circularly symmetric filter $\Psi(\vec{x}; R, \vec{b})$. The filtered field is given by (19). Now, we express the conditions to obtain a filter for the detection of the source $s(x) = A\tau(x)$ at the origin taking into account the fact that the source is characterized by a single scale R_0. We assume the following

conditions:

(1) $\langle w(R_0,\vec{0})\rangle = s(0) \equiv A$, that is, $w(R_0,\vec{0})$ is an *unbiased* estimator of the amplitude of the source;

(2) the variance of $w(R,\vec{b})$ has a minimum at the scale R_0, that is, it is an *efficient* estimator.

Then, the 2D filter satisfying these conditions is the so-called *matched filter*. As mentioned before, we will allow the filter scale to be modified by a factor α. If $\alpha = 1$ we have the well-known standard matched filter use in the literature. For a source with a Gaussian profile, a scale-free power spectrum $P(q) \propto q^{-\gamma}$, and allowing the filter scale to vary through the α parameter, the modified matched filter is

$$\psi_{\mathrm{MF}}(q) = N(\alpha) z^{\gamma} e^{-(1/2)z^2}, \quad z \equiv q\alpha R, \tag{23}$$

where

$$m \equiv \frac{2+\gamma}{2}, \qquad N(\alpha) = \frac{\alpha^2}{\Delta^m}\frac{1}{\pi}\frac{1}{\Gamma(m)}, \quad \Delta = \frac{2\alpha^2}{(1+\alpha^2)}, \tag{24}$$

and Γ is the standard Gamma function. The parameters of the filtered background and source are

$$\rho(\alpha) = \rho = \sqrt{\frac{m}{1+m}}, \qquad \theta_m(\alpha) = \alpha R\sqrt{\frac{2}{1+m}}, \qquad y_s(\alpha) = \rho\Delta. \tag{25}$$

The corresponding threshold as compared to the standard matched filter ($\alpha = 1$) is

$$\frac{\nu(\alpha)}{\nu_{\mathrm{MF}(\alpha=1)}} = \alpha^{t-2}\Delta^m, \tag{26}$$

where

$$t \equiv \frac{2-\gamma}{2}. \tag{27}$$

We remark that for the standard matched filter the curvature does not affect the region of acceptance and the linear detector $\varphi(\nu,\kappa)$ is reduced to $\varphi = \nu$.

4.2. The scale-adaptive filter

The scale-adaptive filter (or optimal pseudo-filter) has been proposed by Sanz et al. [19]. The filter is obtained by imposing an additional condition to the conditions that define the MF:

(3) $w(R,\vec{0})$ has a maximum at $(R_0,\vec{0})$.

Considering a scale-free power spectrum, $P(q) \propto q^{-\gamma}$, a modified scale αR, and a Gaussian profile for the source, the functional form of the filter in 2D is

$$\psi_{\mathrm{SAF}}(q) = N(\alpha) z^{\gamma} e^{-(1/2)z^2}\left[\gamma + \frac{2t}{m}z^2\right], \quad z \equiv q\alpha R, \tag{28}$$

where

$$N(\alpha) = \frac{\alpha^2}{\Delta^m}\frac{1}{\pi\Gamma(m)}\frac{1}{\gamma + (2t/m)\Delta}, \tag{29}$$

and where m and Δ are defined as in (24), t is defined as in (27). The parameters of the filtered background and source are

$$\rho(\alpha) = \rho = \sqrt{\frac{m}{1+m}}\frac{H_1}{\sqrt{H_2 H_3}}, \qquad \theta_m(\alpha) = \alpha R\sqrt{\frac{2}{1+m}}\sqrt{\frac{H_1}{H_3}},$$
$$y_s(\alpha) = \sqrt{\frac{m}{1+m}}\sqrt{\frac{H_2}{H_3}}\Delta\frac{\gamma + c(1+m)\Delta}{\gamma + cm\Delta}, \tag{30}$$

where $c = 2t/m$ and

$$H_1 = \gamma^2 + 2\gamma c(1+m) + c^2(1+m)(2+m),$$
$$H_2 = \gamma^2 + 2\gamma cm + c^2 m(1+m), \tag{31}$$
$$H_3 = \gamma^2 + 2\gamma c(2+m) + c^2(2+m)(3+m).$$

The corresponding threshold as compared to the standard matched filter ($\alpha = 1$) is

$$\frac{\nu}{\nu_{\mathrm{MF}(\alpha=1)}} = \frac{\alpha^{t-2}\Delta^m(\gamma + cm\Delta)}{\sqrt{H_2}}. \tag{32}$$

4.3. The Mexican hat wavelet

The MHW is defined to be proportional to the Laplacian of the Gaussian function in 2D real space

$$\psi_{\mathrm{MHW}}(x) \propto (1-x^2)e^{-(1/2)x^2}, \quad x \equiv |\vec{x}|. \tag{33}$$

Thus, in Fourier space we get the modified Mexican hat wavelet introducing the α parameter as follows:

$$\psi_{\mathrm{MHW}}(q) = N(\alpha) z^2 e^{-(1/2)z^2}, \quad z \equiv q\alpha R,$$
$$N(\alpha) = \frac{1}{\pi}\left(\frac{\alpha}{\Delta}\right)^2. \tag{34}$$

Thus, the filtered background and source parameters are

$$\rho(\alpha) = \rho = \sqrt{\frac{2+t}{3+t}}, \qquad \theta_m(\alpha) = \alpha R\sqrt{\frac{2}{3+t}},$$
$$y_s(\alpha) = \frac{2}{\sqrt{(2+t)(3+t)}}\Delta, \tag{35}$$

where m and Δ are defined as in (24) and t is defined as in (27). The corresponding threshold is

$$\frac{\nu(\alpha)}{\nu_{\mathrm{MF}(\alpha=1)}} = \frac{\alpha^{t-2}\Delta^2}{\sqrt{\Gamma(m)\Gamma(2+t)}}. \tag{36}$$

Table 1: Number density of detections n^* for the BSAF and the standard MF ($\alpha = 1$) with optimal values of c and α for different values of n_b^* and R. RD means relative difference in number densities in percentage: RD $\equiv 100(-1 + n^*_{\mathrm{BSAF}}/n^*_{\mathrm{MF}})$.

R	n_b^*	α	c	n^*_{BSAF}	n^*_{MF}	RD(%)
1.5	0.005	0.5	−0.44	0.0507	0.0484	4.7
	0.01	0.5	−0.46	0.0709	0.0620	14.3
2	0.005	0.4	−0.54	0.0396	0.0335	18.2
	0.01	0.4	−0.54	0.0567	0.0406	39.6
2.5	0.005	0.3	−0.64	0.0320	0.0245	30.6

4.4. The biparametric scale-adaptive filter

López-Caniego et al. [21] have shown that removing condition (3) defining the SAF and introducing instead the condition

(3) $w(R_0, \vec{b})$ has a maximum at $(R_0, \vec{0})$

leads to the new filter

$$\psi(q) \propto \frac{\tau(q)}{P(q)}[1 + c(qR)^2], \tag{37}$$

where c is an arbitrary constant related to the curvature of the maximum. For the case of a scale-free spectrum, and allowing for a modified scale αR, the filter is given by the parameterized equation

$$\begin{aligned} \psi_{\mathrm{BSAF}}(q) &= N(\alpha) z^\gamma e^{-(1/2)z^2}(1 + cz^2), \quad z \equiv q\alpha R, \\ N(\alpha) &= \frac{\alpha^2}{\Delta^m}\frac{1}{\pi}\frac{1}{\Gamma(m)}\frac{1}{1 + cm\Delta}, \end{aligned} \tag{38}$$

where m and Δ are defined as in (24). We remark that $c = 0$ leads to the MF, and if $c \equiv 2t/m\gamma$, with t defined as in (27), the BSAF becomes the SAF. The parameters of the filtered background and source are

$$\begin{aligned} \rho(\alpha) = \rho &= \sqrt{\frac{m}{1+m}}\frac{D_1}{\sqrt{D_2 D_3}}, \qquad \theta_m(\alpha) = \alpha R\sqrt{\frac{2}{1+m}}\sqrt{\frac{D_1}{D_3}}, \\ y_s(\alpha) &= \sqrt{\frac{m}{1+m}}\sqrt{\frac{D_2}{D_3}}\Delta\frac{1 + c(1+m)\Delta}{1 + cm\Delta}, \end{aligned} \tag{39}$$

where

$$\begin{aligned} D_1 &= 1 + 2c(1+m) + c^2(1+m)(2+m), \\ D_2 &= 1 + 2cm + c^2 m(1+m), \\ D_3 &= 1 + 2c(2+m) + c^2(2+m)(3+m). \end{aligned} \tag{40}$$

The equivalent threshold is given by

$$\frac{\nu(\alpha)}{\nu_{\mathrm{MF}(\alpha=1)}} = \frac{\alpha^{t-2}\Delta^m(\gamma + cm\Delta)}{\sqrt{D_3}}. \tag{41}$$

5. ANALYTICAL RESULTS

In this section we will compare the performance of the different filters previously introduced. We use as an example the interesting case of white noise as background. This is a fair approximation to the case presented in Figure 1, where the sources are embedded in a background that is a combination of instrumental noise (approximately Gaussian) and a small contribution of residual foregrounds that have not been perfectly separated. For this example, we will consider sources with intensities distributed uniformly between zero and an upper cutoff.

The comparison of the filters is performed as follows. We fix the number density of spurious detections, the same for all the filters. Then, for any given filter we calculate the quantities σ_n, ρ, and y_s. Using (15) it is possible to calculate the value of φ_* that defines the region of acceptance. Then we calculate the number density of real detections using (16). The filter that leads to the highest number density of detections will be the preferred one. We do this for different values of α in order to test how the variation of the filtering scale affects the number of detections.

5.1. A priori probability distribution

As mentioned before, we will test a pdf of source intensities that is uniform in the interval $0 \le A \le A_c$. In terms of normalized intensities, we have the pdf

$$p(\nu_s) = \frac{1}{\nu_c}, \quad \nu_s \in [0, \nu_c]. \tag{42}$$

We will consider a cutoff in the amplitude of the sources such that $\nu_c = 2$ after filtering with the standard MF, that is, we will focus on the case of faint sources that would be very difficult to detect if no filtering was applied. Note that while the value ν_c is different for each filter (because each filter leads to a different dispersion σ_0 of the filtered field), the distribution in source intensities A is the same for all the cases.

5.2. Results for white noise

We want to find the optimal filter in the sense of the maximum number of detections. For the sources, we use a uniform distribution with amplitudes in the interval $A \in [0, 2]\sigma_0$, where σ_0 is the dispersion of the linearly filtered map with the standard MF. We focus on the interesting case of white noise ($\gamma = 0$) and explore different values of n_b^* and R. The results are summarised in Table 1.

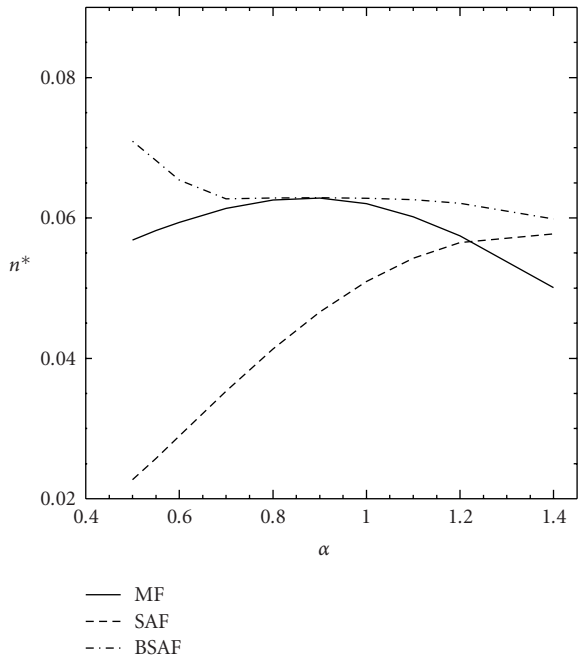

Figure 2: The expected number density of detections n^* as a function of α for $\gamma = 0$ for the BSAF (c has been obtained by maximizing the number of detections for each value of α), MF, and SAF filters. We consider the case $R = 1.5$, $n_b^* = 0.01$.

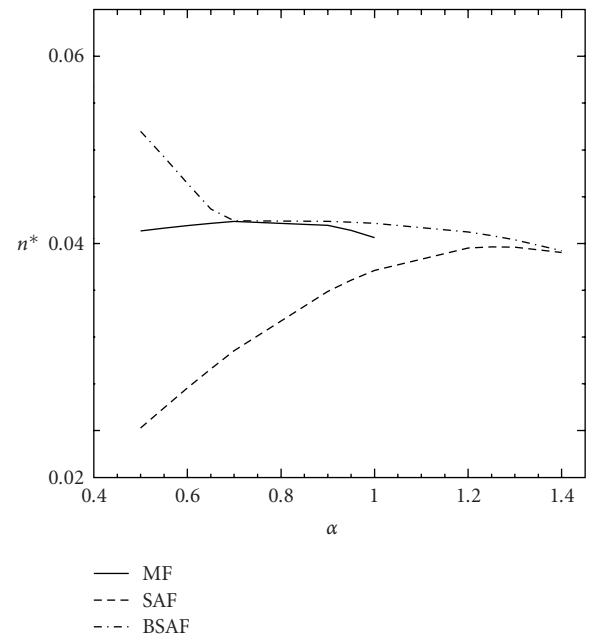

Figure 3: The expected number density of detections n^* as a function of α for $\gamma = 0$ for the BSAF (c has been obtained by maximising the number of detections for each value of α), MF, and SAF filters. We consider the case $R = 2$, $n_b^* = 0.01$.

We study the performance of the different filters as a function of α. This allows us to test how the variation of the natural scale of the filters helps the detection. In the case of the BSAF, which has an additional free parameter, c in (38), for each value of α we determine numerically the value of c that gives the highest number of detections. Then the BSAF with such c parameter (i.e., a function of α, n_b^*, and R) is compared with the other filters.

In Figure 2, we plot the expected number density of detections n^* for different values of α, $R = 1.5$ pixels, and $n_b^* = 0.01$. Note that for the 2D case the MHW and SAF are the same filter for $\gamma = 0$, and we have only included the latter in our figures. In this case, the curve for the BSAF always goes above the other filters. The maximum number of detections is found for small values of α. In this region, the improvement of the BSAF with respect to the standard matched filter is of order $\simeq 15\%$.

In Figure 3, we show the results for $R = 2$. We have increased the beam width as compared to the previous example and left unchanged the number density of false detections. The BSAF outperforms all the other filters, and for small values of α the improvement is of order $\simeq 40\%$. Note that in this figure the MF takes values $\alpha \in [0, 1]$. For greater values of α, with $R = 2$ and $n_b^* = 0.01$, we cannot solve for φ_* in the implicit equation (15) and cannot calculate n^*.

We remark that filtering at scales much smaller than the scale of the pixel does not make sense. This is due to the fact that we are not including the effect of the pixel in our theoretical calculations and, thus, the results would not exactly follow what would be found in a real image. Therefore, we present the results only for those values of α such that αR is at least ~ 1.

6. CONCLUSIONS

Several techniques have been introduced in the literature to detect point sources in two-dimensional images. Examples of point sources in astronomy are far galaxies as detected by CMB experiments. An approach that has been thoroughly used in the literature for this case consists in linear filtering the data and applying detectors based on thresholding. Such approach uses only information on the amplitude of the sources: the potentially useful information contained in the local spatial structure of the peaks is not used at all. In our work, we design a detector based on peak statistics that uses the information contained in the amplitude, curvature, and shear of the maxima. These quantities describe the local properties of the maxima and are used to distinguish statistically between peaks due to background fluctuations and peaks due to the presence of a source.

We derive a Neyman-Pearson detector (NPD) that considers number densities of peaks which leads to a sufficient detector that, in the case of the spherically symmetric sources that we consider, is linear in the amplitude and curvature of the sources. For this particular case, then, the information of the shear of the peaks is not relevant. In other cases, however, it could be useful.

It is a common practice in astronomy to linear filter the images in order to enhance very faint point sources and help the detection. The best filter would be the one that makes it easier to distinguish between peaks coming from the background alone and those due to the presence of a source, according to the information used by the detector. In the case of simple thresholding, which considers only the amplitude of the peaks, the answer to the question of which is the best filter (in the previous sense) is well known: the standard matched filter. But in the case of the Neyman-Pearson detector, which considers other things apart from mere amplitudes, this is no longer true.

We have compared three commonly used filters in the literature in order to assess which one of them performs better when detecting sources with our scheme. In addition, we have designed a filter such that it optimizes the number of true detections for a fixed number of spurious sources. The optimization of the number of true detections is performed by using the a priori pdf of the amplitudes of the sources. This filter depends on two free parameters and it is therefore called biparametric scale-adaptive filter (BSAF). By construction, the functional form of the BSAF includes the standard MF as a particular case and its performance in terms of number of true detections for a fixed number of spurious detections must be at least as good as the standard MF's one.

Following the work done in the 1D case, we generalize the functional form of the filters to 2D and introduce an extra degree of freedom α that will allow us to filter at different scales αR, where R is the scale of the source. This significantly improves the results.

We have considered an interesting case, a uniform distribution of weak sources with amplitudes $A \in [0,2]\sigma_0$, where σ_0 is the dispersion of the field filtered with the standard matched filter, embedded in white noise ($\gamma = 0$). We have tested different values of the source size R and of the number density of spurious detections n_b^* that we fix. We find that the BSAF improves the number density of detections up to $\simeq 40\%$ with respect to the standard MF ($\alpha = 1$) for certain cases. Note that since the Neyman-Pearson detector for the standard MF ($\alpha = 1$) defaults to the classic thresholding detector that is commonly used in astronomy, the results of this work imply that it is possible, under certain circumstances, to detect more point sources than in the classical approach.

The generalization of these ideas to other source profiles and non-Gaussian backgrounds is relevant and will be discussed in a future work.

APPENDIX

We will show in this appendix that $\varphi(\nu,\kappa) \geq \varphi_*$ given in (13) is a sufficient linear detector, that is, the detector is linear in the threshold ν and the curvature κ and the data it uses is a sufficient statistic to decide if a peak is a source (independent of the a priori probability $P(\nu_s)$). The ratio $L(\nu,\kappa,\epsilon|\nu_s) \equiv n(\nu,\kappa,\epsilon|\nu_s)/n_b(\nu,\kappa,\epsilon)$ can be explicitly written as

$$L(\nu,\kappa,\epsilon|\nu_s) = e^{\varphi\nu_s - (1/2)(\nu_s^2 + (\rho\nu_s - 2\kappa_s)^2)}. \tag{A.1}$$

The criterion for detection can be written as

$$Ł(\nu,\kappa) \equiv \int_0^\infty d\nu_s p(\nu_s) L(\nu,\kappa|\nu_s) \geq L_*, \tag{A.2}$$

where L_* is a constant. L is a function of φ,

$$\varphi(\nu,\kappa) \equiv a\nu + b\kappa, \quad a = \frac{1-\rho y_s}{1-\rho^2},\ b = \frac{y_s - \rho}{1-\rho^2}. \tag{A.3}$$

By differentiating L with respect to φ we find that

$$\frac{\partial L}{\partial \varphi} = \int_0^\infty d\nu_s p(\nu_s)\nu_s e^{\varphi\nu_s - (1/2)(\nu_s^2 + (\rho\nu_s - 2\kappa_s)^2)} \geq 0, \tag{A.4}$$

and therefore setting a threshold in L is equivalent to setting a threshold in φ:

$$Ł(\nu,\kappa) \geq L_* \iff \varphi(\nu,\kappa) \geq \varphi_*, \tag{A.5}$$

where $\varphi(\nu,\kappa)$ is given by (A.3) and φ_* is a constant.

ACKNOWLEDGMENTS

The authors thank Patricio Vielva for useful discussions. López-Caniego thanks the Ministerio de Ciencia y Tecnología (MCYT) for a predoctoral FPI fellowship. Barreiro thanks the MCYT and the Universidad de Cantabria for a Ramón y Cajal contract. Herranz acknowledges support from the European Community's Human Potential Programme under contract HPRN-CT-2000-00124, CMBNET, and from an ISTI fellowship since September 2004. We acknowledge partial support from the Spanish MCYT project ESP2002-04141-C03-01 and from the EU Research Training Network "Cosmic Microwave Background in Europe for Theory and Data Analysis."

REFERENCES

[1] C. Baccigalupi, L. Bedini, C. Burigana, et al., "Neural networks and separation of cosmic microwave background and astrophysical signals in sky maps," *Monthly Notices of the Royal Astronomical Society*, vol. 318, no. 3, pp. 769–780, 2000.

[2] D. Maino, A. Farusi, C. Baccigalupi, et al., "All-sky astrophysical component separation with fast independent component analysis (FASTICA)," *Monthly Notices of the Royal Astronomical Society*, vol. 334, no. 1, pp. 53–68, 2002.

[3] J. Delabrouille, J. F. Cardoso, and G. Patanchon, "Multidetector multicomponent spectral matching and applications for cosmic microwave background data analysis," *Monthly Notices of the Royal Astronomical Society*, vol. 346, no. 4, pp. 1089–1102, 2003.

[4] L. Bedini, D. Herranz, E. Salerno, C. Baccigalupi, E. E. Kuruoğlu, and A. Tonazzini, "Separation of correlated astrophysical sources using multiple-lag covariance matrices," *EURASIP Journal on Applied Signal Proccessing*, vol. 2005, no. 15, pp. 2400–2412, 2005, Special issue on applications of signal processing in astrophysics and cosmology.

[5] M. P. Hobson, A. W. Jones, A. N. Lasenby, and F. R. Bouchet, "Foreground separation methods for satellite observations of the cosmic microwave background," *Monthly Notices of the Royal Astronomical Society*, vol. 300, no. 1, pp. 1–29, 1998.

[6] F. R. Bouchet and R. Gispert, "Foregrounds and CMB experiments I. Semi-analytical estimates of contamination," *New Astronomy*, vol. 4, no. 6, pp. 443–479, 1999.

[7] V. Stolyarov, M. P. Hobson, M. A. J. Ashdown, and A. N. Lasenby, "All-sky component separation for the Planck mission," *Monthly Notice of the Royal Astronomical Society*, vol. 336, no. 1, pp. 97–111, 2002.
[8] R. B. Barreiro, M. P. Hobson, A. J. Banday, et al., "Foreground separation using a flexible maximum-entropy algorithm: an application to COBE data," *Monthly Notices of the Royal Astronomical Society*, vol. 351, no. 2, pp. 515–540, 2004.
[9] L. Toffolatti, F. Argüeso, G. De Zotti, et al., "Extragalactic source counts and contributions to the anisotropies of the cosmic microwave background: predictions for the Planck Surveyor mission," *Monthly Notices of the Royal Astronomical Society*, vol. 297, no. 1, pp. 117–127, 1998.
[10] B. Guiderdoni, E. Hivon, F. R. Bouchet, and B. Maffei, "Semi-analytic modelling of galaxy evolution in the IR/submm range," *Monthly Notices of the Royal Astronomical Society*, vol. 295, no. 4, pp. 877–898, 1998.
[11] M. Tucci, E. Martínez-González, L. Toffolatti, J. González-Nuevo, and G. De Zotti, "Predictions on the high-frequency polarization properties of extragalactic radio sources and implications for polarization measurements of the cosmic microwave background," *Monthly Notices of the Royal Astronomical Society*, vol. 349, no. 4, pp. 1267–1277, 2004.
[12] M. P. Hobson, R. B. Barreiro, L. Toffolatti, et al., "The effect of point sources on satellite observations of the cosmic microwave background," *Monthly Notices of the Royal Astronomical Society*, vol. 306, no. 1, pp. 232–246, 1999.
[13] L. Cayón, J. L. Sanz, R. B. Barreiro, et al., "Isotropic wavelets: a powerful tool to extract point sources from cosmic microwave background maps," *Monthly Notices of the Royal Astronomical Society*, vol. 315, no. 4, pp. 757–761, 2000.
[14] P. Vielva, E. Martínez-González, L. Cayón, J. M. Diego, J. L. Sanz, and L. Toffolatti, "Predicted Planck extragalactic point-source catalogue," *Monthly Notices of the Royal Astronomical Society*, vol. 326, no. 1, pp. 181–191, 2001.
[15] P. Vielva, R. B. Barreiro, M. P. Hobson, et al., "Combining maximum-entropy and the Mexican hat wavelet to reconstruct the microwave sky," *Monthly Notices of the Royal Astronomical Society*, vol. 328, no. 1, pp. 1–16, 2001.
[16] P. Vielva, E. Martínez-González, J. E. Gallegos, L. Toffolatti, and J. L. Sanz, "Point source detection using the Spherical Mexican Hat Wavelet on simulated all-sky Planck maps," *Monthly Notices of the Royal Astronomical Society*, vol. 344, no. 1, pp. 89–104, 2003.
[17] M. Tegmark and A. de Oliveira-Costa, "Removing point sources from cosmic microwave background maps," *The Astrophysical Journal Letters*, vol. 500, no. 2, pp. L83–L86, 1998.
[18] L. Y. Chiang, H. E. Jørgensen, I. P. Naselsky, P. D. Naselsky, I. D. Novikov, and P. R. Christensen, "An adaptive filter for the PLANCK compact source catalogue construction," *Monthly Notices of the Royal Astronomical Society*, vol. 335, no. 4, pp. 1054–1060, 2002.
[19] J. L. Sanz, D. Herranz, and E. Martínez-González, "Optimal detection of sources on a homogeneous and isotropic background," *The Astrophysical Journal*, vol. 552, no. 2, pp. 484–492, 2001.
[20] D. Herranz, J. L. Sanz, R. B. Barreiro, and E. Martínez-González, "Scale-adaptive filters for the detection/separation of compact sources," *The Astrophysical Journal*, vol. 580, no. 1, pp. 610–625, 2002.
[21] M. López-Caniego, D. Herranz, R. B. Barreiro, and J. L. Sanz, "A Bayesian approach to filter design: detection of compact sources," in *Computational Imaging II*, vol. 5299 of *Proceedings of SPIE*, San Jose, Calif, USA, January 2004.
[22] M. López-Caniego, J. L. Sanz, D. Herranz, and R. B. Barreiro, "Filter design for the detection of compact sources based on the Neyman-Pearson detector," *Monthly Notices of the Royal Astronomical Society*, vol. 359, pp. 993–1006, 2005.
[23] S. O. Rice, "Mathematical analyses of random noise," in *Selected Papers on Noise and Stochastic Processes*, N. Wax, Ed., Dover Publications, New York, NY, USA, 1954.
[24] J. R. Bond and G. Efstathiou, "The statistics of cosmic background radiation fluctuations," *Monthly Notices of the Royal Astronomical Society*, vol. 226, pp. 655–687, 1987.
[25] R. B. Barreiro, J. L. Sanz, E. Martínez-González, L. Cayón, and J. Silk, "Peaks in the cosmic microwave background: flat versus open models," *The Astrophysical Journal*, vol. 478, part 1, no. 1, pp. 1–6, 1997.

M. López-Caniego received his M.S. degree in physics from the Universidad Autonoma de Madrid, Madrid, Spain, in 2000, after completing as part of his degree one year at the University of Frankfurt, Germany. He was a Research Fellow at Bell Labs, Lucent Technologies, New Jersey, USA, during 2001, before he continued his postgraduate studies at the Universidad Autonoma de Madrid in 2002. At the end of this year he joined a research group at the Instituto de Fisica de Cantabria (CSIC-UC), where he is currently pursuing his Ph.D. in the field of image processing under an MCYT FPI predoctoral fellowship. His research interests are in the areas of gravitational lensing and cosmic microwave background astronomy and the development and application of statistical signal processing techniques to astronomical data, in particular, linear and nonlinear filtering for the detection and extraction of extragalactic point sources.

D. Herranz received the B.S. degree in 1995 and the M.S. degree in 1995 from the Universidad Complutense de Madrid, Madrid, Spain, and the Ph.D. degree in astrophysics from Universidad de Cantabria, Santander, Spain, in 2002. He was a CMBNET Postdoctoral Fellow at the Istituto di Scienza e Tecnologie dell'Informazione "A. Faedo" (CNR), Pisa, Italy, from 2002 to 2004. He is currently at the Instituto de Fisica de Cantabria, Santander, Spain, under an MEC Juan de la Cierva contract. His research interests are in the areas of cosmic microwave background astronomy and extragalactic point source statistics as well as the application of statistical signal processing to astronomical data, including blind source separation, linear and nonlinear data filtering, and statistical modeling of heavy-tailed processes.

J. L. Sanz received the M.S. degree in 1971 from the Universidad Complutense de Madrid, Spain, and the Ph.D. degree in physical sciences from Universidad Autonoma de Madrid, Spain, in 1976. He was a Postdoctoral Fellow at the Queen Mary College, London, UK, during 1978. He is currently Professor of astrophysics at the Instituto de Fisica de Cantabria, Santander, Spain. His research interests are in the areas of cosmic microwave background astronomy (extragalactic point sources, component separation, and non-Gaussian studies) as well as the application of statistical signal processing and image analysis to astronomical data (linear and nonlinear data filtering, fusion).

R. B. Barreiro obtained her B.S. degree in 1995 from the Universidad de Santiago de Compostela, Spain, completing also as part of her degree one year at the University of Sheffield, UK. She completed her Ph.D. in astrophysics in the Universidad de Cantabria in 1999. After her Ph.D., she worked as a Research Associate at the Cavendish Laboratory of the University of Cambridge, UK, until the end of 2001. She is currently at the Instituto de Fisica de Cantabria (CSIC-UC), Spain, under a Ramón y Cajal contract. Her research interests are mainly focused in the field of the cosmic microwave background, including statistical data analysis, in particular the study of the Gaussianity of the CMB, and the development of component separation techniques for both diffuse emissions and compact sources.